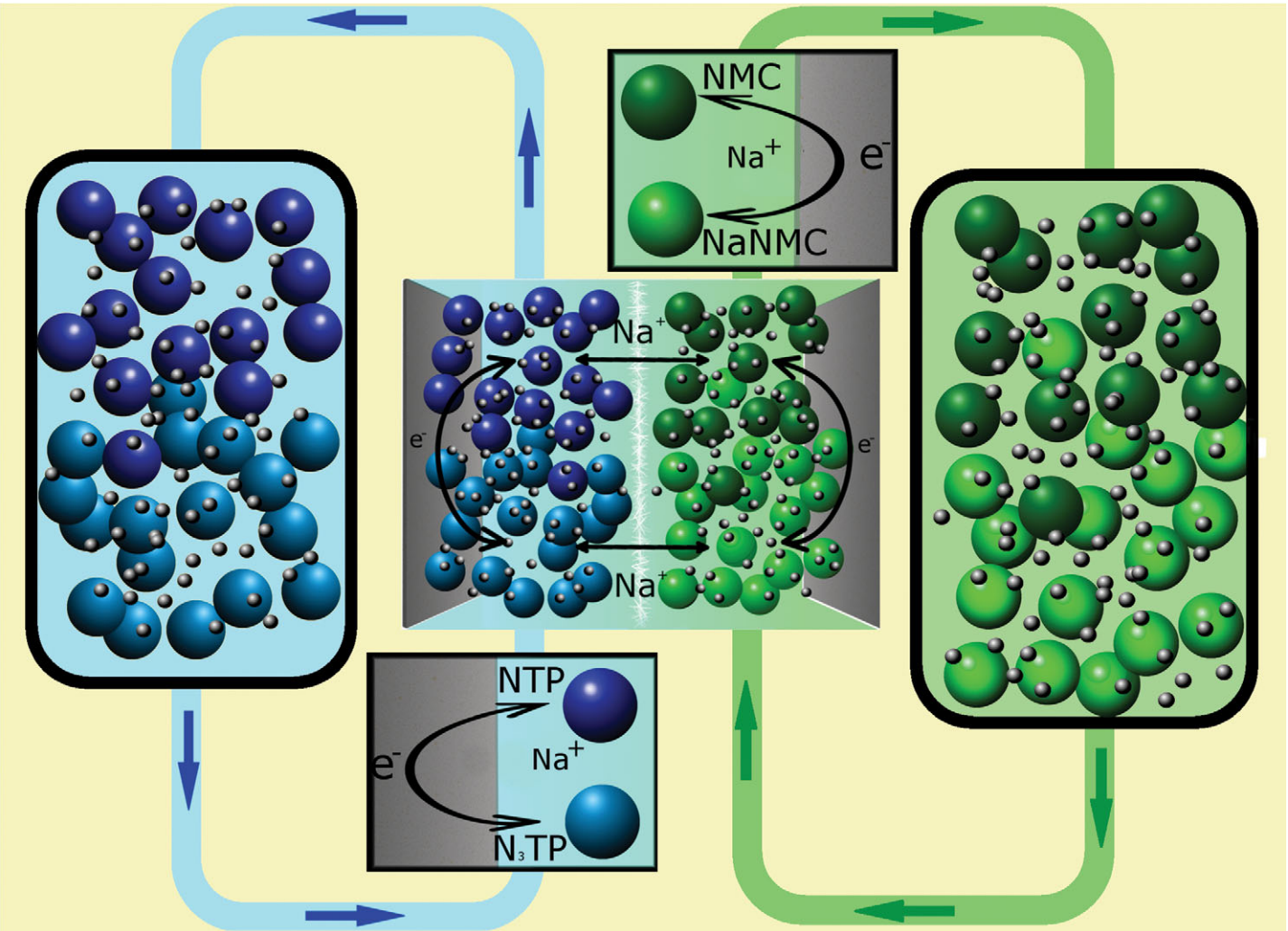

Showcasing research from Dr Edgar Ventosa at the Catalonia Institute for Energy Research, Barcelona, Spain

Non-aqueous semi-solid flow battery based on Na-ion chemistry. P2-type $Na_xNi_{0.22}Co_{0.11}Mn_{0.66}O_2$–$NaTi_2(PO_4)_3$

A proof of concept for non-aqueous Na-ion semi-solid flow battery is demonstrated. This concept opens the door for developing a new low-cost type of non-aqueous semi-solid flow batteries based on the rich chemistry of Na-ion intercalating compounds.

As featured in:

See Edgar Ventosa *et al.*, *Chem. Commun.*, 2015, **51**, 7298.

ROYAL SOCIETY OF CHEMISTRY

www.rsc.org/chemcomm

Registered charity number: 207890

ChemComm

COMMUNICATION

View Article Online
View Journal | View Issue

Cite this: *Chem. Commun.*, 2015, 51, 7298

Received 1st December 2014,
Accepted 22nd December 2014

DOI: 10.1039/c4cc09597a

www.rsc.org/chemcomm

Non-aqueous semi-solid flow battery based on Na-ion chemistry. P2-type $Na_xNi_{0.22}Co_{0.11}Mn_{0.66}O_2$–$NaTi_2(PO_4)_3$†

Edgar Ventosa,*[a] Daniel Buchholz,[bcd] Stefan Klink,[e] Cristina Flox,[a] Luciana Gomes Chagas,[bcd] Christoph Vaalma,[bc] Wolfgang Schuhmann,[e] Stefano Passerini[bc] and Joan Ramon Morante[af]

We report the first proof of concept for a non-aqueous semi-solid flow battery (SSFB) based on Na-ion chemistry using P2-type $Na_xNi_{0.22}Co_{0.11}Mn_{0.66}O_2$ and $NaTi_2(PO_4)_3$ as positive and negative electrodes, respectively. This concept opens the door for developing a new low-cost type of non-aqueous semi-solid flow batteries based on the rich chemistry of Na-ion intercalating compounds.

Redox flow batteries (RFB) are promising technologies for energy storage due to the long life, low cost, high round-trip efficiency and independent scalability of energy and power capabilities.[1–6] Semi-solid flow batteries (SSFBs) are a special class of RFB, in which anolyte and catholyte consist of flowable suspensions of solid active materials rather than dissolved redox species.[7–11] Thus, the concentration of active redox centres in the anolyte and catholyte of the SSFB can be significantly increased. Using intercalation type active materials such as those typically used in Li-ion batteries (LIBs), *e.g.* $Li_4Ti_5O_{12}$, $LiCoO_2$ or $LiNi_{0.5}Mn_{1.5}O_4$, the energy densities can reach up to 300–500 W h L^{-1}, which is more than 10 times higher than that of all-vanadium RFBs (40 W h L^{-1}).[7] Compared to LIBs, SSFBs present several advantages: (I) power and energy can be scaled independently, (II) the amount of inactive materials such as current collectors or housing is decreased, and (III) the manufacturing processes become simpler and more cost-effective.

Sodium-ion batteries (SIBs) attracted increasing attention in the past few years since sodium is abundant, inexpensive, and does not alloy with aluminium which allows for cheaper current collectors.[12–14] Energy densities of *ca.* 200 W h kg^{-1} have been proposed to be achievable.[14] Even more importantly, while sodium intercalation compounds do not necessarily exhibit similar performance like their lithium counterparts, sodium does offers an even larger variety of crystal chemistries than lithium. As such, SIB technology is still considered to be in its infancy, and new active materials are developed.[15,16]

A key aspect in both LIB and SIB is the formation of the so called solid electrolyte interphase on negative (SEI) and positive (CEI) electrodes operated outside the electrochemical stability window due to reductive or oxidative decomposition of the carbonate based electrolyte. In the case of SSFBs, the formation of these passivating films has a specific detrimental effect since it hinders the electrical connection between the current collector and single particles dispersed in the electrolyte. In consequence, Duduta *et al.*[7] employed $Li_4Ti_5O_{12}$ as negative electrode material since it operates above the reduction potential of carbonate electrolytes to construct the first proof of principle of non-aqueous Li-ion SSFB. For SIBs, however, the search for "SEI-free" negative electrodes is more difficult, since the intercalation of sodium into the analogues of $Li_4Ti_5O_{12}$ or TiO_2 does not operate within the stability window of the electrolyte.[17,18]

The NASICON material $NaTi_2(PO_4)_3$ (NaTP), however, does operate at a very flat potential plateau located at around *ca.* 2.1 V *vs.* Na/Na^+,[19–21] which is well above the stability limit of typical electrolytes.[22] As it can be seen from Fig. 1a, a charge capacity of 125 mA h g^{-1} can be utilized when cycled as solid film electrode *versus* metallic sodium in a three-electrode Swagelok cell, which is very close to the theoretical value of 133 mA h g^{-1}.

The positive electrode material should likewise operate at high potentials just below the potential of electrolyte oxidation. As shown in Fig. 1b, P2-type $Na_xNi_{0.22}Co_{0.11}Mn_{0.66}O_2$ (NaNCM) has been demonstrated to store reversibly *ca.* 130 mA h g^{-1} in the range 4.3–2.1 V with excellent cyclibility.[23–25] Detailed structural characterization of NaTP and NaNCM is given in the ESI.† On the base of the electrochemical performances of these materials, we selected NaTP and NaNCM as negative and positive electrode

[a] *Catalonia Institute for Energy Research, Jardins de les Dones de Negre, e1, 08930 Sant Adria de Besos, Barcelona, Spain. E-mail: edgar.ventosa@rub.de*
[b] *Helmholtz Institute Ulm (HIU) Electrochemistry I, Helmholtzstrasse 11, 89081 Ulm, Germany*
[c] *Karlsruhe Institute of Technology (KIT), P.O. Box 3640, 76021 Karlsruhe, Germany*
[d] *Institute of Physical Chemistry, University of Muenster, Corrensstrasse 28/30, Muenster, 48149, Germany*
[e] *Analytical Chemistry – Center for Electrochemical Sciences (CES), Ruhr-University Bochum, Universitätsstr. 150, 44780 Bochum, Germany*
[f] *Departament d'Electronica, Facultat de Fisica, Universitat de Barcelona, Martí i Franques 1, 08028 Barcelona, Spain*

† Electronic supplementary information (ESI) available: Experimental details, XRD patterns, SEM images. See DOI: 10.1039/c4cc09597a

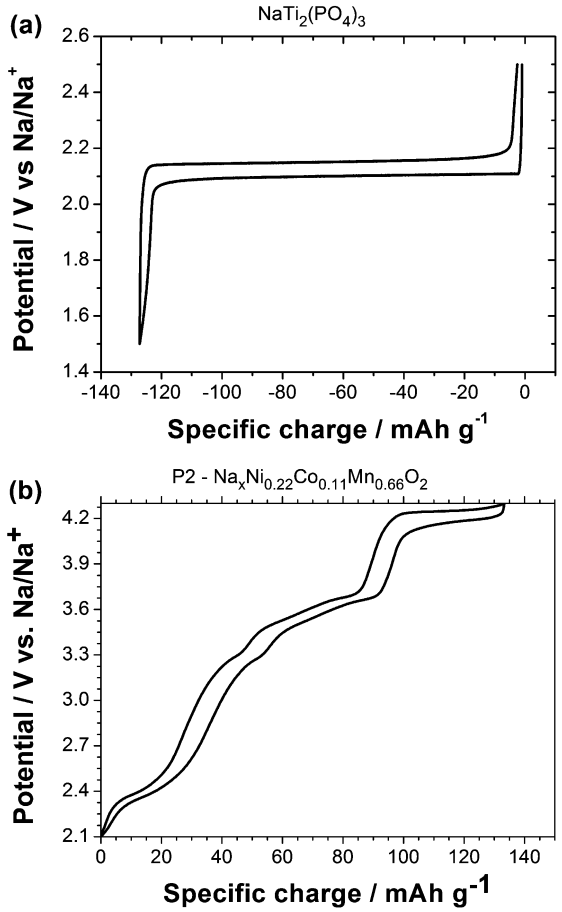

Fig. 1 Potential profile of (a) carbon coated (2 wt%) $NaTi_2(PO_4)$ and (b) P2-type $Na_xNi_{0.22}Co_{0.11}Mn_{0.66}O_2$ in the second cycle at 0.1C (12 mA g^{-1}) as solid electrodes. Electrolyte solutions: (a) 1 M $NaClO_4$ in PC, (b) 1 M $NaPF_6$ in PC. Three-electrode Swagelok cell in which the counter and reference electrode was metallic sodium. Temperature: 22 °C.

material for the construction of a non-aqueous sodium-based SSFB.

In the semi-solid flow cell configuration, NaTP and NaNCM were, together with 1.3 wt% conductive additive, dispersed in 0.5 M $NaPF_6$ in ethyl carbonate/dimethyl carbonate (EC:DMC) as anolyte and catholyte. As already suggested before, SSFB are best evaluated under intermittent flow.[7] Although NaTP was expected to be the charge limiting electrode due to the slightly smaller total charge capacity, it is apparent from Fig. 2 that the system was limited by the positive electrode, since the upper cut-off voltage of the battery was reached before reaching the end of the potential plateau of NaTP. Galvanostatic Intermittent Titration Technique (GITT) revealed that overpotentials during charge and discharge (*ca.* 0.5 V) at a current density of 0.5 mA cm^{-2} (*ca.* 0.35 C) mostly derive from the ohmic overpotential at the positive electrode, which prevents most of the suspension from accessing the charge capacity observed in solid electrode above 4.0 V.

Decreasing the current density to 0.17 mA cm^{-2} (*ca.* 0.1 C), indeed, resulted in a significantly improved specific charge capacity of the suspensions (Fig. 3). Fig. 3a shows the voltage profiles of three subsequent cycles for the first injection. A reversible specific

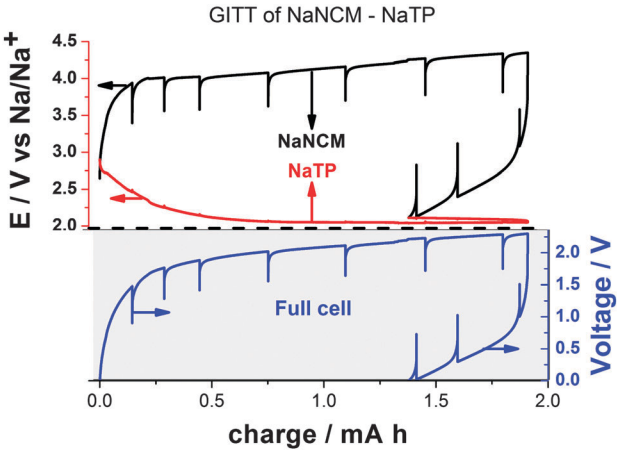

Fig. 2 GITT potential curves of the SSFB consisting of suspensions of P2-type $Na_xNi_{0.22}Co_{0.11}Mn_{0.66}O_2$–C/$NaTi_2(PO_4)_3$ (positive and negative electrodes, respectively) at 0.5 mA cm^{-2} (*ca.* 0.35 C) in static. The upper part displays the potentials profiles of the positive and negative electrode *versus* a reference of Na/Na^+, and the bottom part depicts the resulting voltage of the battery.

charge capacity of *ca.* 80 mA h $g_{cathode}^{-1}$ was obtained for the first three cycles demonstrating the good reversibility of the electrochemical processes. The reversible charge capacity of the suspension (80 mA h g_{NaNCM}^{-1}) was below the value obtained using the solid electrode (130 mA h g_{NaNCM}^{-1}) which is likely due to the fact that the charge capacity of NaNCM above 4.0 V *vs.* Na/Na^+ (Fig. 1) was not accessible due to high overpotentials.

The coulombic efficiency increased from 53% to 86–88% after the first cycle. The reduction of surface groups of carbon at the negative electrode as well as some electrolyte decomposition at the positive side occurring mainly during the first cycle were assumed to be the source of the observed modulation in efficiency. The differential voltage plot (Fig. 3b) indicates that the charge process occurred mainly in voltage regions located at around 1.9 V, whereas the discharge started at 1.35 V, reached the maximum at 1.1 V and then continues to the lower cut-off voltage. Increasing the upper cut-off voltage from 2.2 V to 2.3 V led to an increment in the reversible specific charge of 8 mA h g_{NaNCM}^{-1}. On the other hand, the coulombic efficiency decreased from 88% to 84%, which was probably related with electrolyte decomposition at the positive electrode. This suggests that upper cut-off voltages above 2.2 V are not suitable. Fig. 3d depicts the voltage profiles of three subsequent injections of suspensions. Between the injections, the suspensions were flown for at least 10 min (at 3 mL min^{-1} for a total volume of 6 mL of suspension) to homogenize the entire suspension. The fifth cycle of the first injection is included for comparison. An increase of 15 mA h g_{NaNCM}^{-1} was observed from the first to the second injection and it stabilized from the second to the third one. The decrease of irreversible processes and an improved electrical percolation of the suspensions after several days of stirring were possibly responsible for the increase of reversible specific charge.

The coulombic efficiency of the first cycle increased from the first to subsequent injections (53%, 79% and 75% for 1st, 2nd and 3rd injection, respectively). Nevertheless, the values of coulombic

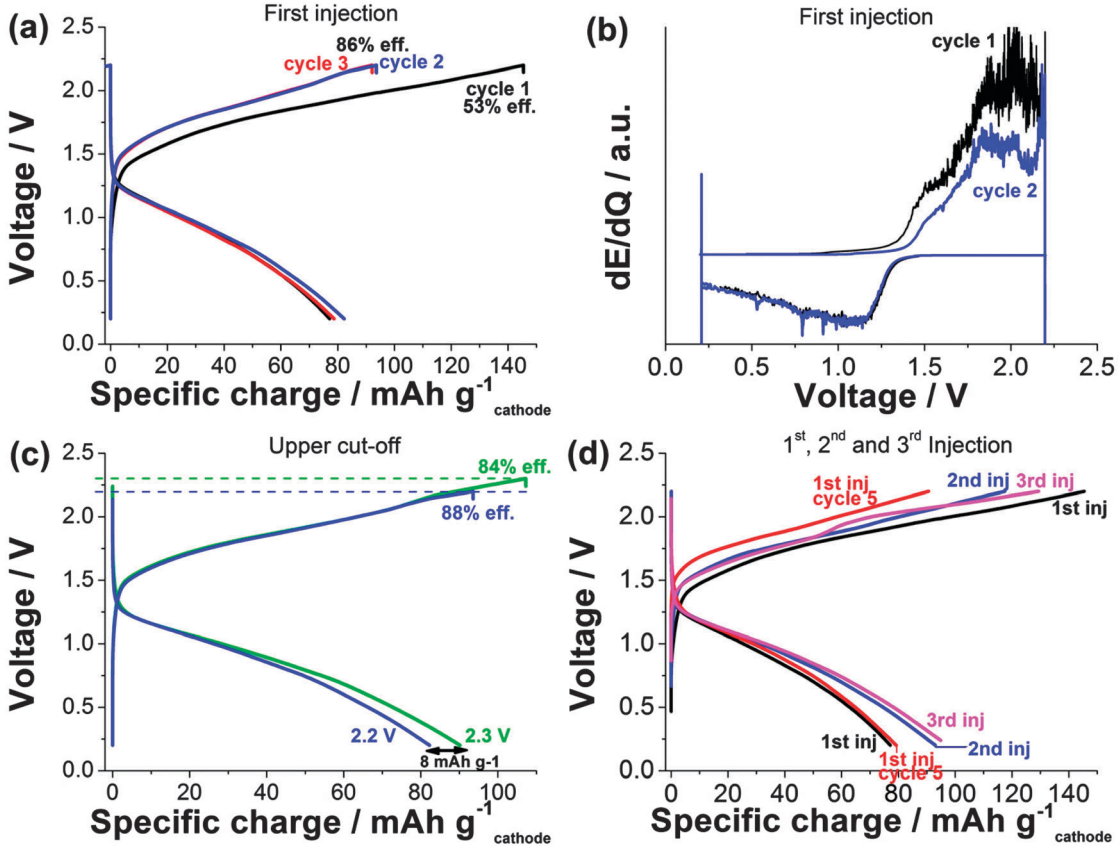

Fig. 3 (a) Voltage profiles of the first three cycles of the first injection of SSFB consisting of suspensions of P2-type $Na_xNi_{0.22}Co_{0.11}Mn_{0.66}O_2$–C/$NaTi_2(PO_4)_3$ (positive and negative electrodes, respectively) at 0.17 mA cm^{-2} in static (*ca.* 65 mg of active material in the anolyte and catholyte compartments). (b) Differential voltage plot of the first injection. (c) Voltage profiles of the first injection with two different upper cut-off voltages (2.2 V and 2.3 V). (d) Voltage profiles of the first cycle of the three first injections as well as the fifth cycle of the first injection.

efficiency of the first cycle of the second and third injection were in between those of the first and the fifth cycle of the first injection (53% and 88%, respectively). In other words, (i) the amount of irreversible processes occurring in the first injection decreases for subsequent injections (2nd, 3rd, *etc.*) and (ii) the amount of irreversible processes occurring in the fifth cycle of the first injection is lower than that of the first cycle of subsequent fresh injections. This fact indicates that irreversible processes decrease after the first injection for each fresh injection and they continue decreasing until the entire volume of suspension has been cycled. On the other hand, the coulombic efficiency even after several cycles remained rather low (88%), which suggests that the voltage limit of 2.2 V to be slightly too high and electrolyte decomposition to occur, especially if the large active material-electrolyte contact area and the values obtained for Li-based SSFB (80% coulombic efficiency in the second cycle) are taken into account.[7]

In conclusion, we have successfully demonstrated that non-aqueous semi-solid flow batteries can operate on Na-ion based chemistry. This first proof of principle has been achieved by employing P2-type $Na_xNi_{0.22}Co_{0.11}Mn_{0.66}O_2$ and $NaTi_2(PO_4)_3$ as positive and negative electrode materials, respectively. The proposed battery stores 80 mA h g_{NaNCM}^{-1} within the voltage range of 2.2–0.2 V. First results are encouraging but certainly indicate the need for a better understanding and control of irreversible charge losses in this type of battery. Although the energy density of this proof of concept was *ca.* 9 W h L^{-1} (6 W h kg^{-1}), a proper selection and optimization of the electrolyte, active materials, especially the negative electrode, as well as cycling conditions will certainly result in a significantly improved electrochemical performance of sodium-based SSFBs, *e.g.* a 2.5 V battery with 30 vol% of active material in the suspensions would deliver *ca.* 150 W h L^{-1}.

The research leading to these results has received funding from the European Union Seventh Framework Programme (FP7/2007–2013) under grant agreement no. 608621. European Regional Development Funds (ERDF-FEDER Programa Competitivitat de Catalunya 2007–2013) are also acknowledged.

Notes and references

1 Z. G. Yang, J. L. Zhang, M. C. W. Kintner-Meyer, X. C. Lu, D. W. Choi, J. P. Lemmon and J. Liu, *Chem. Rev.*, 2011, **111**, 3577–3613.
2 C. P. de Leon, A. Frias-Ferrer, J. Gonzalez-Garcia, D. Szanto and F. C. Walsh, *J. Power Sources*, 2006, **160**, 716–732.
3 L. Joerissen, J. Garche and C. Fabjan, *J. Power Sources*, 2004, **127**, 98–104.
4 M. Skyllas-Kazacos and F. Grossmith, *J. Electrochem. Soc.*, 1987, **134**, 2950–2953.
5 C. Flox, M. Skoumal, J. Rubio-Garcia, T. Andreu and J. R. Morante, *Appl. Energy*, 2013, **109**, 344–351.
6 C. Flox, J. Rubio-Garcia, R. Nafria, R. Zamani, M. Skoumal, T. Andreu, J. Arbiol, A. Cabot and J. R. Morante, *Carbon*, 2012, **50**, 2372–2374.

7 M. Duduta, B. Y. Ho, V. C. Wood, P. Limthongkul, V. E. Brunini, W. C. Carter and Y.-M. Chiang, *Adv. Energy Mater.*, 2011, **1**, 511–516.
8 S. Hamelet, T. Tzedakis, J.-B. Leriche, S. Sailler, D. Larcher, P.-L. Taberna, P. Simon and J.-M. Tarascon, *J. Electrochem. Soc.*, 2012, **159**, A1360–A1367.
9 Y. Yang, G. Zheng and Y. Cui, *Energy Environ. Sci.*, 2013, **6**, 1552–1558.
10 S. Hamelet, D. Larcher, L. Dupont and J.-M. Tarascon, *J. Electrochem. Soc.*, 2013, **160**, A516–A520.
11 F. Y. Fan, W. H. Woodford, Z. Li, N. Baram, K. C. Smith, A. Helal, G. H. McKinley, W. C. Carter and Y.-M. Chiang, *Nano Lett.*, 2014, **14**, 2210–2218.
12 M. D. Slater, D. Kim, E. Lee and C. S. Johnson, *Adv. Funct. Mater.*, 2013, **23**, 947–958.
13 S.-W. Kim, D.-H. Seo, X. Ma, G. Ceder and K. Kang, *Adv. Energy Mater.*, 2012, **2**, 710–721.
14 H. Pan, Y.-S. Hu and L. Chen, *Energy Environ. Sci.*, 2013, **6**, 2338–2360.
15 M. Dahbi, N. Yabuuchi, K. Kubota, K. Tokiwa and S. Komaba, *Phys. Chem. Chem. Phys.*, 2014, **16**, 15007–15028.
16 H. Pan, Y.-S. Hu and L. Chen, *Energy Environ. Sci.*, 2013, **6**, 2338.
17 Y. Sun, L. Zhao, H. Pan, X. Lu, L. Gu, Y.-S. Hu, H. Li, M. Armand, Y. Ikuhara, L. Chen and X. Huang, *Nat. Commun.*, 2013, **4**, 1870.
18 L. Wu, D. Bresser, D. Buchholz, G. Giffin, C. Ramirez-Castro, A. Ochel and S. Passerini, *Adv. Energy Mater.*, DOI: 10.1002/aenm.201401142.
19 Z. Li, D. Young, K. Xiang, W. C. Carter and Y.-M. Chiang, *Adv. Energy Mater.*, 2013, **3**, 290–294.
20 C. Delmas, A. Nadiri and J. L. Soubeyroux, *Solid State Ionics*, 1988, **28–30**, 419–423.
21 S. Patoux and C. Masquelier, *Chem. Mater.*, 2002, **14**, 5057–5068.
22 A. Bhide, J. Hofmann, A. K. Dürr, J. Janek and P. Adelhelm, *Phys. Chem. Chem. Phys.*, 2014, **16**, 1987–1998.
23 D. Buchholz, A. Moretti, R. Kloepsch, S. Nowak, V. Siozios, M. Winter and S. Passerini, *Chem. Mater.*, 2013, **25**, 142–148.
24 D. Buchholz, L. Gomes Chagas, M. Winter and S. Passerini, *Electrochim. Acta*, 2013, **110**, 208–213.
25 L. Gomes Chagas, D. Buchholz, L. Wu, B. Vortmann and S. Passerini, *J. Power Sources*, 2014, **247**, 377–383.